Computational and Structural Biotechnology Journal 27 (2025) 1112–1123

Contents lists available at ScienceDirect

Computational and Structural Biotechnology Journal

journal homepage: www.elsevier.com/locate/csbj

Research article

Directed disruption of IL2 aggregation and receptor binding sites produces designer biologics with enhanced specificity and improved production capacity☆

Amy Dashwood [a,b,1], Ntombizodwa Makuyana [a,b,1], Rob van der Kant [c,d,1], Arman Ghodsinia [a], Alvaro R. Hernandez [a,e], Stephanie Lienart [b], Oliver Burton [a,b], James Dooley [a,b], Magda Ali [a], Lubna Kouser [b], Francisco Naranjo [b], Matthew G. Holt [c,d,f], Frederic Rousseau [c,d], Joost Schymkowitz [c,d], Adrian Liston [a,b,*]

[a] Department of Pathology, University of Cambridge, Cambridge, United Kingdom
[b] Immunology Programme, The Babraham Institute, Cambridge, United Kingdom
[c] KU Leuven, Leuven, Belgium
[d] VIB Center for Brain and Disease Research, Leuven, Belgium
[e] Department of Life Sciences, Imperial College London, London, United Kingdom
[f] Instituto de Investigação e Inovação em Saúde (i3S), University of Porto, Porto, Portugal

ARTICLE INFO

Keywords:
Interleukin-2
Cytokine
Protein engineering

ABSTRACT

The pleotropic nature of interleukin-2 (IL2) has allowed it to be used as both a pro-inflammatory and anti-inflammatory therapeutic agent, through promotion of regulatory T cell (Treg) responses via the trimeric IL2RABG receptor or promotion of CD8 T cell responses via the dimeric IL2RBG receptor, respectively. However, the utility of IL2 as a treatment is limited by this same pleiotropy, and protein engineering to bias specificity towards either Treg or CD8 T cell lineage often requires a trade-off in protein production or total bioactivity. Here we use SolubiS and dTANGO, computational algorithm-based methods, to predict mutations within the IL2 structure to improve protein production yield in muteins with altered cellular selectivity, to generate combined muteins with elevated therapeutic potential. The design and testing process identified the V106R (murine) / V91R (human) mutation as a Treg-enhancing mutein, creating a cation repulsion to inhibit primary binding to IL2RB, with a post-IL2RA confirmational shift enabling secondary IL2RB binding, and hence allowing the trimeric receptor complex to form. In human IL2, additional N90R T131R aggregation-protecting mutations could improve protein yield of the V91R mutation. The approach also generated novel CD8 T cell-promoting mutations. Y59K created a cation-cation repulsion with IL2RA, while Q30W enhanced CD8 T cell activity through potential π-stacking enhancing binding to IL2RB, with the combination highly stimulatory for CD8 T cells. For human IL2, Y45K (homolog to murine Y59K) coupled with E62K prevented IL2RA binding, however it required the aggregation-protecting mutations of N90R T131R to rescue production. These muteins, designed with both cellular specificity and protein production features, have potential as both biological tools and therapeutics.

1. Introduction

Interleukin 2 (IL2) is a highly potent cytokine, capable of both maintaining homeostasis and driving inflammatory reactions [1]. These dual functions are based on the differential expression of the different receptor complexes. The high affinity receptor, a trimer of IL2RA, IL2RB and ILR2G (CD25, CD122, CD132, respectively), is dominantly expressed by regulatory T cells (Tregs), allowing IL2 to control Treg

☆ Directed disruption of aggregation-prone linear segments of IL2 produces designer biologics with enhanced therapeutic potential.

* Corresponding author at: Department of Pathology, University of Cambridge, Cambridge, United Kingdom.
E-mail addresses: al989@cam.ac.uk (A. Dashwood), al989@cam.ac.uk (A. Liston).

[1] equal contribution

https://doi.org/10.1016/j.csbj.2025.03.002
Received 12 November 2024; Received in revised form 28 February 2025; Accepted 1 March 2025
Available online 4 March 2025

homeostasis through effects on Treg "fitness" and proliferation/apoptosis control [2–5]. The intermediate affinity receptor, a dimer of IL2RB and ILR2G, is expressed by cells with more inflammatory potential, largely CD8 T cells and NK cells. Due to the ~100-fold lower affinity of the dimer for IL2, at normal levels of IL2 production the dominant role is to establish homeostasis [6,7]. Elevated IL2 production is, however, among the earliest events following CD4 T cell activation [8], supporting the proliferation of CD8 T cells and NK cells during an immune reaction. This response is aided by transient low-level upregulation of IL2RA on responding cells, providing an inflammatory interlude before homeostasis is re-established through the Treg response to elevated IL2 [7]. This dominant IL2 network is further complicated by context-dependent IL2 circuits [9] and alterations of receptor expression during pathology [10,11].

With the immunological capacity to both elevate tolerogenic (Treg) and immunogenic (CD8 T cell/NK) responses, IL2 is a highly attractive therapeutic target. The clinical utility is, however, limited by the concentration-dependent effects, especially as the half-life of IL2 is around 5 minutes following injection [12,13]. Multiple approaches to engineer more stable concentrations have been developed, including modification of IL2 through post-translational modification, such as PEGylation [14,15], via fusion to protein carriers, such as the immunoglobulin Fc region [16–18] or a soluble version of the IL2RA protein [19], or through sustained production using gene therapy vectors [20]. Additionally, a single mutation K35E, identified through screening of a phage-display library, has been shown to increase secretion levels of designer IL2 biologics by up to 20 fold, increasing production yield [21]. An alternative approach has been to decouple this concentration-dependent effect by restricting function to either the trimeric or dimeric receptor, through either screening/*in vitro* evolution approaches [22] or rational design [23,24]. IL2 muteins can be created with alterations to the IL2RA, IL2RB or IL2RG binding interfaces, including enhanced binding to IL2RA [25], reduced binding to IL2RA [26], increased binding to IL2RB [22,23,27]; reduced IL2RB binding [28,29] or reduced activation of the receptor complex via IL2RG [24,30–32]. The net effects are designer IL2 variants with increased selectivity for Tregs, increased selectivity for CD8 T cells and NK cells, or antagonistic activity, depending on which binding structure is disrupted. IL2 variants combining both elevated longevity and altered specificity have also been generated, such as combining an IL2 mutein with an Fc fusion [33,34], or targeting PEGylation to a particular IL2 interface [15]. Finally, more exotic approaches have been used, including the *de novo* design of protein capable of binding only one surface of the IL2R [35], or the creation of IL2/IL2R orthogonal pairs that do not cross-react with the native system [36].

While IL2 muteins provide enhanced specificity for either the Treg or CD8 T cell lineage, depending on the mutation design, a feature commonly observed in muteins is reduced stability or bioactivity [27,28,34,37]. As either of these attributes limit the utility of the mutein in biotechnology, we sought to design novel IL2 mutations using the SolubiS algorithm, which enables rational design of mutations to enhance stability, and dTANGO for targeted disruption of receptor binding. Using this system, we designed and validated families of IL2 mutations with enhanced specificity for either Tregs or CD8 T cells, while maintaining total bioactivity and maintaining or even improving production capacity. This combination of features provides potential utility for these muteins in clinical therapeutics.

2. Results

2.1. Directed disruption of IL2 aggregation and receptor biding sites

A key limitation in the production capacity of proteins is the aggregation of nascent polypeptides, mediated through aggregation-prone hydrophobic stretches [38]. As protein-protein binding sites are frequently hydrophobic, this feature allows the potential for the design of mutations that both disrupt a protein-protein interaction and also improve protein production through lowering the aggregation rates [39]. To improve the properties of IL2, we designed a series of mutations in both human and mouse IL2. Mutation design was based on the structure of the human and murine IL2 structures, and used the SolubiS method [40] to provide maximal improvements to aggregation resistance with minimal point mutations. Stability of protein folding, protein-receptor interactions and aggregation propensity were further predicted using FoldX and TANGO resulting values were scored against thresholds. Candidate mutations which had a reduction in TANGO score by more than 100, did not destabilise hIL2 (ddG <0.5 Kcal/mol) and did not disturb receptor interactions (ddG <0.5 Kcal/mol) except where desired were taken forward into functional testing (Table 1). A full list of the predicted biochemical properties of each mutein is listed in Supplementary Spreadsheet 1.

Table 1
IL2 muteins design strategy.

Organism	Mutation	# of mutations	Human homolog	Strategy
Human	N90R	1	-	SolubiS monomer
Human	N90E	1	-	SolubiS monomer
Human	T123N	1	-	SolubiS monomer
Human	T131R	1	-	SolubiS monomer
Human	H16W	1	-	Kill IL2RB binding
Human	D20R	1	-	Kill IL2RB binding
Human	N88H	1	-	Kill IL2RB binding
Human	V91R	1	-	Kill IL2RB binding
Human	N90R T123N	2	-	SolubiS combo
Human	N90R T131R	2	-	SolubiS combo
Human	V91R T123N	2	-	SolubiS with kill IL2RB binding
Human	N88H T131R	2	-	SolubiS with kill IL2RB binding
Human	E62K	1	-	Kill IL2RA binding
Human	Y45K	1	-	Kill IL2RA binding
Human	Y45K E62K	2	-	Kill IL2RA binding
Human	Y45K E62K N90E	3	-	SolubiS with kill IL2RA binding
Human	Y45K E62K N90E T131R	4	-	SolubiS with kill IL2RA binding
Mouse	A138N	1	T123N	SolubiS monomer
Mouse	T146R	1	T131R	SolubiS monomer
Mouse	Q30W	1	H16W	Kill IL2RB binding
Mouse	D34R	1	D20R	Kill IL2RB binding
Mouse	N103H	1	N88H	Kill IL2RB binding
Mouse	V106R	1	V91R	Kill IL2RB binding
Mouse	V106R A138N	2	V91R T123N	SolubiS with kill IL2RB binding
Mouse	N103H T146R	2	N88H T131R	SolubiS with kill IL2RB binding
Mouse	E76K	1	E62K	Kill IL2RA binding
Mouse	Y59K	1	Y45K	Kill IL2RA binding
Mouse	Y59K E76K	2	Y45K E62K	Kill IL2RA binding
Mouse	Y59K E76K A138N	3	Y45K E62K N90E	SolubiS with kill IL2RA binding
Mouse	Y59K E76K T146K	3	Y45K E62K N90E T131R	SolubiS with kill IL2RA binding

2.2. Production screening of IL2 muteins identifies point mutations with improved production capacity

To functionally test the designed IL2 mutations, we first screened for production capacity of each mutein, through cloning the IL2 muteins into an expression plasmid transfected into HEK293 cells. Through normalisation of IL2 protein production (measured through ELISA for a His tag fused to the C terminus of each protein) to HEK293 transfection efficiency (measured through PCR quantification of expression plasmid), we could compare the production output of each mutein relative to wildtype IL2. For the mutations in murine IL2, muteins T116R, V106R A138N, and Y59K resulted in a trend towards elevated IL2 production, up to ~3-fold higher than wildtype IL2 levels, while other mutants gave equivalent or worse production (Fig. 1**A**). For the mutation in human IL2, muteins N90R T123N, V91R T123N trended towards increased production but no mutants gave significantly elevated production, and several had production defects (Fig. 1**B**). The combination of N90R T131R with Y45K E62K resulted in a rescue of production ($p=0.055$) equivalent to wildtype levels, whilst the Y45K E62K mutation on its own resulted in a markedly reduced production (Fig. 1**B**).

2.3. SolubiS murine IL2 muteins have altered cellular specificity

To determine the impact of these IL2 mutations on receptor specificity, we used a functional assay based on detection of signalling within murine Tregs or CD8 T cells. Using phospho-STAT5 (pSTAT5) as the readout for receptor triggering in both Tregs and CD8 T cells, following incubation in a mixed murine splenocyte population, activation was assessed by flow cytometry. Of the murine mutations designed to prevent binding to IL2RA (E76K and Y59K), both demonstrated reduced pSTAT5 activation in Tregs alone and in combination (Fig. 2**A**). In the case of Y59K, this indicated reduced bioactivity on Tregs. E76K, by contrast, also had production issues and was, therefore, tested at suboptimal doses (0.3 ng/ml), with the poorer pSTAT5 activation potentially reflecting this fact. Of the murine mutations designed to prevent binding to IL2RB (Q30W, D34R, N103H, V106R), Q30W and V106R had preserved activity on Tregs, while D34R and N103H had reduced activity on Tregs (Fig. 2**A**), indicating the latter two mutations had off-target detrimental effects (although in the case of N103H, this may alternatively be attributed to suboptimal production (5.9 ng/ml)). For the effects on CD8 T cells, V106R, V106R A138N and N103H T146R combined normal Treg stimulation with the predicted loss-of-signalling on CD8 T cells, while Q30W had an unexpected major gain-of-signalling effect on CD8 T cells compared to the computational prediction of reduced interaction with IL2RB (Fig. 2**B**). The Y59K mutation retained CD8 T cell stimulation, while having impaired Treg stimulation (Fig. 2**A, B**), consistent with impeded IL2RA binding. Residues designed to boost production, A138N and T146R, were neutral to cell selectivity (Fig. 2**A, B**).

From the initial screen, three murine mutations warranted detailed functional analysis: Y59K, V106R and Q30W. To determine the relative bioactivity of these muteins on Tregs and CD8 T cells, we used the same pSTAT5 response assay, across a titrated dose range, providing

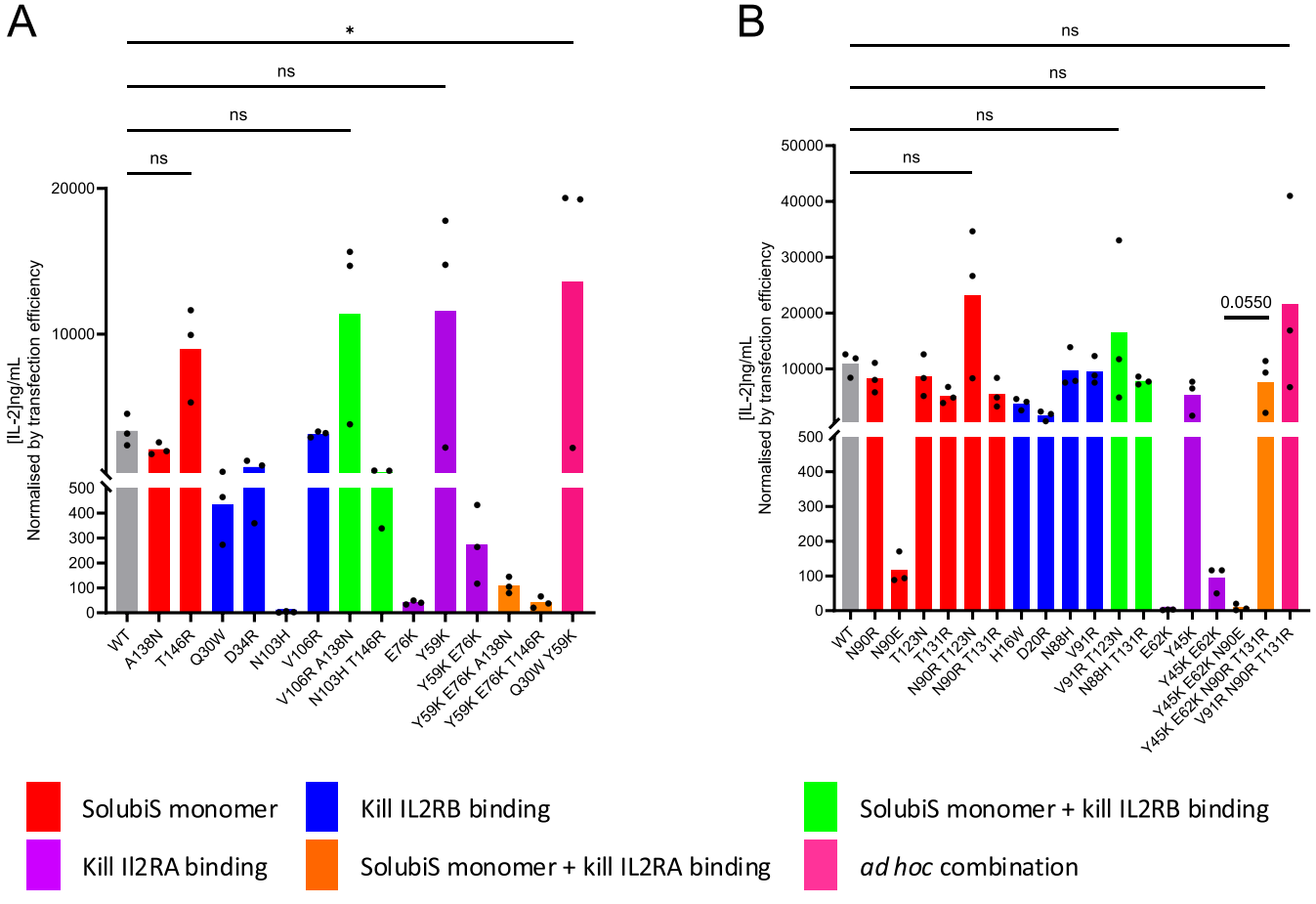

Fig. 1. Screening of IL2 muteins identifies muteins with increased production capacity. A) Murine IL2 mutein production in mammalian HEK293 cells detected via HisTag ELISA and normalised to transfection efficiency measured by qPCR (n=3). B) Human IL2 mutein production in mammalian expression system HEK293 detected via HisTag ELISA and normalised to transfection efficiency measured by qPCR (n=3). Comparisons made using One-Way ANOVA (*P < 0.05, **P < 0.01, ***P < 0.001, **** P<0.0001).

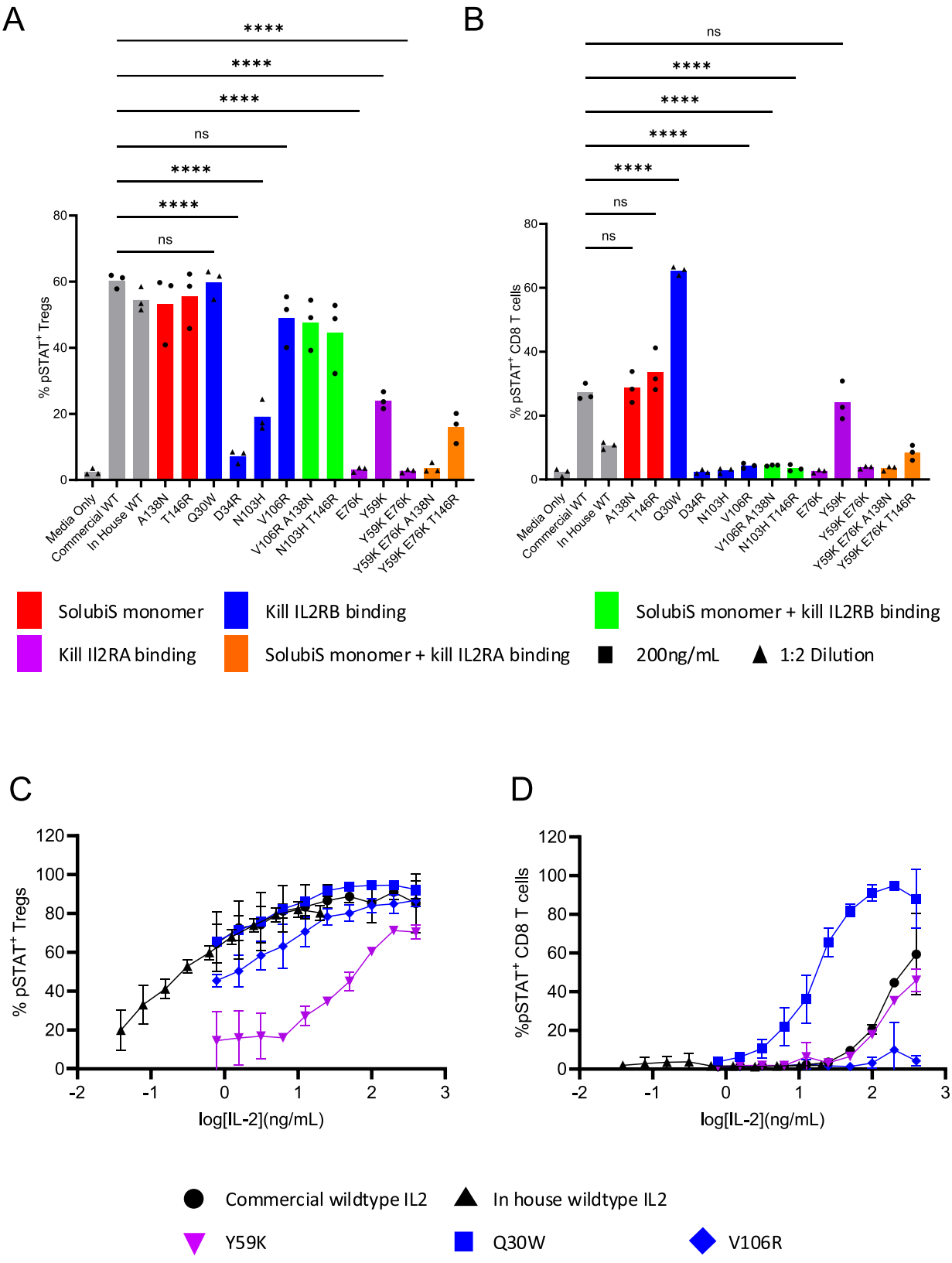

Fig. 2. Altered cellular responses to murine SolubiS IL2 muteins. A) Mouse splenocytes were incubated for 20 minutes with either media containing 200 ng/ml IL2 or 200 ng/ml murine mutein, prior to staining for pSTAT5. For muteins with poor production, where ELISA detected less than 200 ng/ml, a 1:2 dilution of the production supernatant was used instead. The percentage of $pSTAT5^{+}$ cells within the Treg or B) CD8 T cell populations (n=3). Comparisons made using One-Way ANOVA (*P < 0.05, **P < 0.01, ***P < 0.001, **** P<0.0001). C) Mouse splenocytes were incubated for 20 minutes with either media containing IL2 or murine mutein, using a serial dilution of IL2 concentration, prior to staining for pSTAT5. The percentage of $pSTAT5^{+}$ cells within the Treg or D) CD8 T cell populations (n=3).

enhanced sensitivity for detection of functional changes. Compared to both commercial IL2 and the wildtype IL2 control, Y59K demonstrated a >300 fold reduction in activity on Tregs (Fig. 2**C**), while maintaining normal activity on CD8 T cells (Fig. 2**D**), consistent with the designed defect in IL2RA binding. The reverse was observed for V106R (designed for defective IL2RB binding), with normal activity on Tregs (Fig. 2**C**), but no detectable effect on CD8 T cells, even at high doses (Fig. 2**D**). As identified in the functional screening assay, Q30W demonstrated an unexpected effect: normal activity on Tregs (Fig. 2**C**), but strongly elevated effects (~100-fold increased activity) on CD8 T cells (Fig. 2**D**). Together, these results indicate Y59K results in CD8 T cell-specific signalling, V106R results in Treg-specific signalling, and Q30W acts as an unexpected CD8 T cell superkine.

In order to identify the potential mechanism by which Q30W displayed an unexpected increase in activity on CD8 T cells compared to *in silico* predictions, we modelled the effects of the three mutations on murine IL2 / IL2R binding, using a structure built on the human homologs (Fig. 3**A**). First, for Y59K, when modelled as bound to the trimeric IL2R, the native Y79 residue of IL2 is in close proximity to positive charges on the R35 and R36 residues of IL2RA (Fig. 3**B**), consistent with a cation–π interaction. The replacement of this residue by Y59K creates a cation-cation repulsion, consistent with a loss of binding to IL2RA. For the V106R mutein, as the IL2RB interface of IL2 changes conformation after it binds IL2RA, we modelled the complex in the presence and absence of IL2RA. In the unbound state of IL2, the V106R residue would occupy the same space as R41/R42 on IL2RB, creating a direct cation repulsion effect (Fig. 3**C**). However, following binding to IL2RA, IL2 changes conformation in the helix C on which V106R lies, a conformational change that was previously postulated to prime recruitment of IL2RB into the trimeric receptor complex [41]. This conformational change pulls back the V106R residue, reducing the direct cation-cation clash (Fig. 3**C**). This is consistent with the observed poor activation through the dimeric IL2RB/IL2RG complex, but unimpeded activation through the trimeric IL2RA/IL2RB/IL2G complex. Finally, the Q30W mutation was modelled as the analogue to the human H16W, based on the human IL2/IL2R structure. While the H16W mutation was predicted to disrupt the interaction, based on the crystal structure of the complex, Q30W was initially only checked for its effect on the stability of the monomer. Subsequent modelling of the mouse complex revealed the Q30W side chain falls within a hydrophobic groove of IL2RB with potential π-stacking interactions with F101 and F135 residues (Fig. 3**D**). The larger hydrophobic side-chain may, therefore, enhance binding, providing preferred signalling through IL2RB, however crystal structure data would be required to verify this interaction.

2.4. *In vivo functional testing of V106R IL2 mutein*

As proof-of-principle for the utility of the developed IL2 muteins for *in vivo* use, we sought to test the Treg-promoting V106R IL2 mutein in

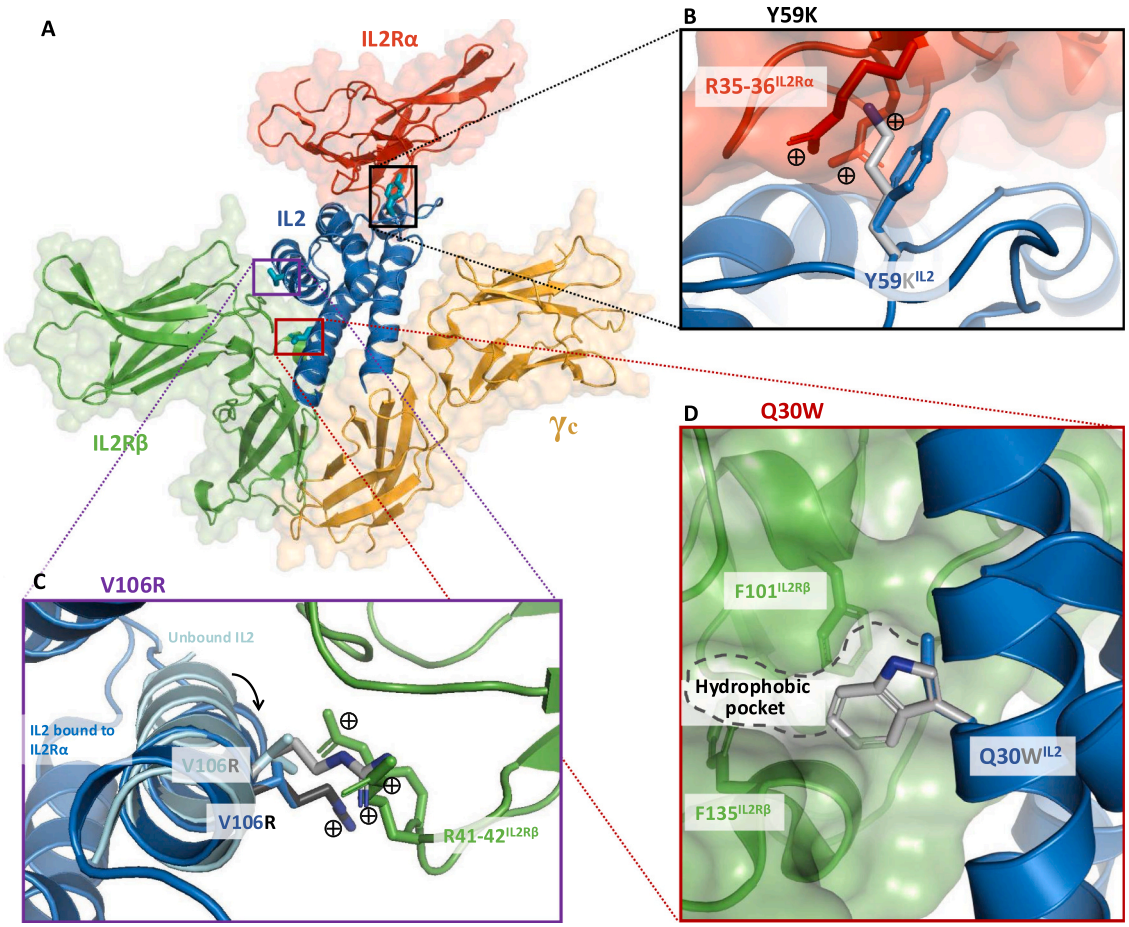

Fig. 3. Structural modelling of murine IL2 muteins with the trimeric IL2R complex. A) Structure of IL2 in complex with the IL2RA/IL2RB/IL2RG trimeric complex, indicating the sites of the three mutated residues. B) The Y59K IL2 mutation, with close proximity to the R25-R26 residues in IL2RA. C) The V106R IL2 mutation, in relation to the R41-R42 residues in IL2RB. The structure of IL2 is shown based on both the unbound IL2 structure and the conformation of IL2 present in the IL2-IL2RA complex, indicating the rotation of the helix from which the V106R side-chain emerges. D) The Q30W IL2 mutation, in relation to the hydrophobic groove present between the F101 and F134 residues of IL2RB. Hydrophobicity in IL2RB represented by colour, with increasing intensity of green representing increasingly hydrophilic values.

mice. We used an AAV-based system (AAV6.2 capsid and a club cell-specific promoter) for transgene delivery into the lung epithelium, (Fig. 4**A**). Transduced cells, expressing the appropriate transcription factors to activate the delivered *Scgb1a1* promoter, are able to drive the production of IL2 in the lung tissue, without giving systemic IL2 production (manuscript in preparation). The system results in rapid production of IL2, with free IL2 levels dropping as IL2-consuming cells build up (Fig. 4**B**). The V106R IL2 mutein built up at higher initial levels than the wildtype IL2 (Fig. 4**B**), consistent with improved stability or a restriction in the number of IL2-consuming cells expanded. The expression of wildtype IL2 in the lung increased the number of lung Tregs, while Tregs in other tissues remained normal (Fig. 4**C**). The V106R IL2 mutein demonstrated a similarly restricted expression profile, producing a further elevation in Treg numbers compared to wildtype IL2 (Fig. 4**C**). This was achieved without expansion of the resident CD8 T cell population, although as no off-target CD8 T cell expansion was observed at this delivery dose even for wildtype IL2 (Fig. 4**D**), it was undetermined whether the V106R mutein also improved specificity or only improved delivery capacity. *Combinatorial generation of a CD8 T cell superkine*

The muteins Q30W and Y59K both demonstrated different desirable properties as a CD8 T cell-promoting IL2 mutant. Q30W increased CD8 T cell signalling, while Y59K boosted production and impeded Treg signalling (Fig. 2**C,D**). To determine if we could engineer a CD8 T cell superkine with all three properties, we sought to combine these mutations. Combination of Q30W Y59K rescued the mild production defect of Q30W, giving a similar production boost to that achieved by Y59K alone (Fig. 1**A**). Upon titration, the Q30W Y59K mutant showed decreased Treg responses by ~30 fold compared to both wildtype and Q30W alone (Fig. 5**A**), giving a defect intermediate to that observed with Y59K. In CD8 T cells, responses to Q30W Y59K, mimicked that of Q30W (Fig. 5**B**). The combination of Q30W Y59K therefore creates a cytokine with the ideal properties of the two parental mutants, with improved production, enhanced CD8 T cell responsiveness and impeded Treg responsiveness.

2.5. SolubiS human IL2 muteins have altered cellular specificity

Similar to the murine muteins, to determine the impact of the human IL2 mutations on receptor specificity, we first used a functional assay based on detection of signalling within human Tregs or CD8 T cells in mixed PBMCs. Of the mutations designed to prevent IL2 binding to the IL2RB (H16W, D20R, N88H, V91R), two of the mutations (D20R, N88H) performed poorly, with detrimental impacts on the pSTAT5 response in Tregs (Fig. 6**A**). This suggests these muteins have a net defect in bioactivity due to poor recruitment of IL2RB to the IL2/IL2RA complex, potentially exacerbated by poor production (D20R=70.83 ng/ml, N88H = 7.65 ng/ml). Three muteins, H16W, V91R and N88H T131R, by contrast, achieved the desired properties of maintained near-normal pSTAT5 responsiveness in Tregs, while also having a sharply reduced signal in CD8 T cells (Fig. 6**B**). Notably, the V91R mutein is the human homolog of V106R, for which the structural modelling suggests IL2/IL2RA complex binding may be rescued by a conformational shift in the mutein residue (Fig. 3**C**). For the residues designed to boost production, N90R, T123N and T131R had neutral effects on Treg signalling, although T123N was detrimental when combined with mutations designed to impede IL2RB binding (Fig. 6**A**). The H16W, V91R and N88H T131R muteins were therefore candidates as Treg-promoting muteins, with poor IL2RB signalling, with V91R having marginally the best production of the three. This production was improved above wildtype values through *ad hoc* combination with N90R T131R, the SolubiS mutation with the best initial production values (Fig. 1**B**).

Of the muteins designed to prevent binding to IL2RA (E62K, Y45K, Y45K E62K) all three modestly reduced Treg responses as designed (Fig. 6**A**). However, E62K and Y45K also did not produce pSTAT5 responses in CD8 T cells, potentially due to production issues lowering their concentration in the assay (E62K = 10.9 ng/ml, Y45K = 9.5 ng/ml) (Fig. 6**B**), making them less useful as candidate cytokines. Interestingly, the combined Y45K E62K mutein stimulated marked responses in CD8 T cells despite production issues (used at a concentration 6-fold

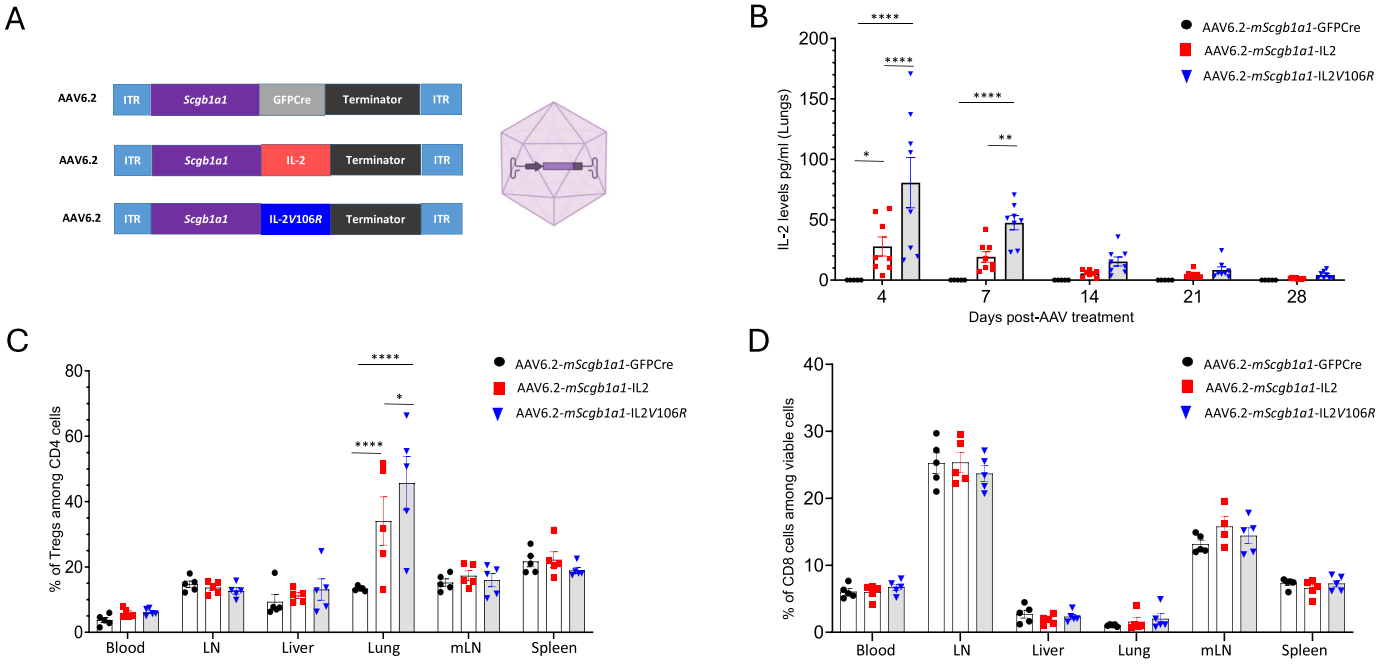

Fig. 4. *In vivo* testing of V106R IL2 enhances local Treg expansion. IL2 and IL2 mutein were delivered *in vivo* using AAV-mediated gene delivery. A. Schematic representation of the viral vector used. Expression is driven by the *Scgb1a1* (Secretoglobin 1A1) promoter and flanked by the inverted terminal repeats. The expression cassette was contained within an AAV6.2 capsid which displays enhanced trophism for lung epithelial cells: AAVs were administrated through the intranasal route (n=5–7 mice/group). B. Available IL2 protein levels in the lung on days 4, 7, 14, 21 and 28 post-AAV delivery. C. Tissues were removed on day 14 and assessed via flow cytometry for the frequency of Foxp3+ Tregs within the CD4+ T cell population, and D. CD8 T cells within the viable cell population. All the data were analysed using Two Way Anova.

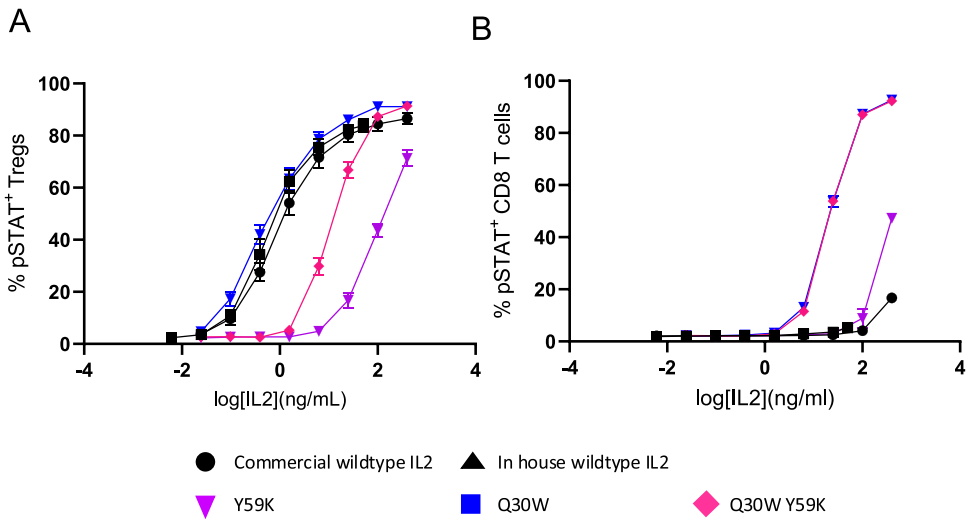

Fig. 5. Combining mutations Q30W and Y59K enhances CD8 T cell selectivity of murine IL2. A) Mouse splenocytes were incubated for 20 minutes with either media containing IL2 or murine mutein, using a serial dilution of IL2 concentration, prior to staining for pSTAT5. The percentage of pSTAT5$^+$ cells within the Treg or B) CD8 T cell populations (n=3).

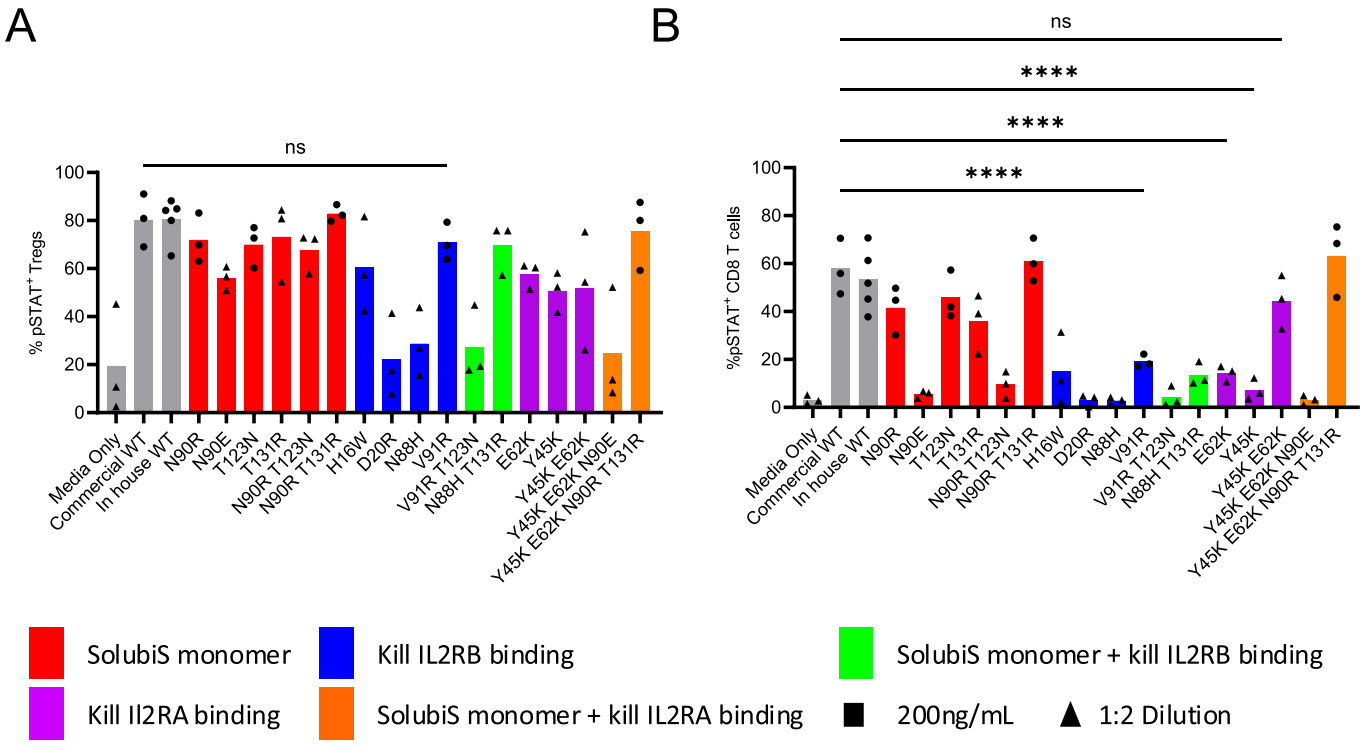

Fig. 6. Altered cellular responses to human SolubiS IL2 muteins. A) Human PBMCs were incubated for 20 minutes with either media containing 200 ng/ml human mutein or 1:2 dilution (where ELISA detected less than 200 ng/ml), prior to staining for pSTAT5. The percentage of pSTAT5$^+$ cells within the Treg or B) CD8 T cell populations (n=3). Comparisons made using One-Way ANOVA (*P < 0.05, **P < 0.01, ***P < 0.001, **** P<0.0001).

less than wildtype, 30.4 ng/ml) (Fig. 6**B**). The Y45K E62K mutation therefore met the biological requirements for a CD8 T cell-promoting mutein, although its relatively poor production would impede therapeutic use. Fortunately, we found that while N90R T131R in isolation demonstrated no increase in production, when in combination with Y45K E62K it rescued the marked defect in production caused by the Y45K E62K mutation and so it was decided to take forward Y45K E62K N90R T131R (Fig. 1**B**).

In addition to the screening performed on human PBMCs, human IL2 variants were also tested on mouse splenocytes to assess cross-reactivity. Whilst WT hIL2 has been shown to cross-react with the mouse IL2 receptor [42] it is crucial to check cross reactivity as this will become important in preclinical safety and toxicity testing. The hIL2 variants tested here showed sufficient cross reactivity to *ex vivo* mouse cells with some attenuated effects in CD8 T cells (Supplementary Figure 1).

2.6. Combination mutants result in human IL2 muteins with enhanced cellular selectivity

Based on this biological characterisation, four human muteins were

of interest for further testing: V91R of particular interest for potential Treg specificity, and the V91R N90R T131R combination with boosted production; Y45K E62K, of particular interest for potential CD8 T cell specificity, and the Y45K E62K N90R T131R production-boosted version. We therefore characterised these four cytokines in the PBMC pSTAT assay for titrated responses to Treg and CD8 T cell activation.

For the potential Treg-boosting V91R and V91R N90R T131R muteins, a titration of the muteins on human PBMCs had intact pSTAT responses in Tregs down to 10 ng/ml, with a drop-off compared to wildtype IL2 at lower concentrations (Fig. 7**A**). In contrast, CD8 T cell responses were muted ~100-fold, even at the highest doses tested (Fig. 7**B**). These results confirm that the V91R mutein, like the analogous V106R mouse mutein, has enhanced specificity for Tregs while maintaining near normal bioactivity.

For the potential CD8 T cell-selective muteins, Y45K E62K and Y45K E62K N90R T131R, production runs were tested in the same PBMC pSTAT assay. In titrations, both the Y45K E62K and Y45K E62K N90R T131R muteins showed sharply diminished Treg responses (~3000 fold) (Fig. 7**C**). In contrast, CD8 T cell responses were akin to wildtype (Fig. 7**D**), demonstrating strong CD8 T cell selectivity. The response curves for Treg and CD8 T cells were highly similar (Fig. 7**C,D**), suggesting near-complete elimination of IL2RA binding and activation of Tregs only through the IL2RB-IL2RG complex, as in CD8 T cells. When also considering the enhanced production values of this mutein (Fig. 1**B**), overall, it shows a superior profile in CD8 T cell-stimulation.

3. Discussion

Protein solubility is adapted to endogenous protein abundance in the cell, where protein folding occurs within the context of specific chaperones and potential interaction partners. For use in biotechnology or therapeutics, proteins require production in recombinant incubators, typically in cell types distinct from those in which they are naturally produced and frequently at concentrations that are several orders of magnitude above their physiological concentration. This often results in protein aggregation, reducing the total protein production yield and increasing costs, creating barriers in affordability and therefore availability of these drugs for patients. Aggregation is a complex process, influenced by physicochemical parameters such as protein and ion concentrations, pH, and temperature, making it challenging to identify sequences that will aggregate under native conditions. The solution to this challenge lies in the distinction between aggregation-prone regions that are thermodynamically protected by folding and those that occur in aggregation-competent conformations that can form without major

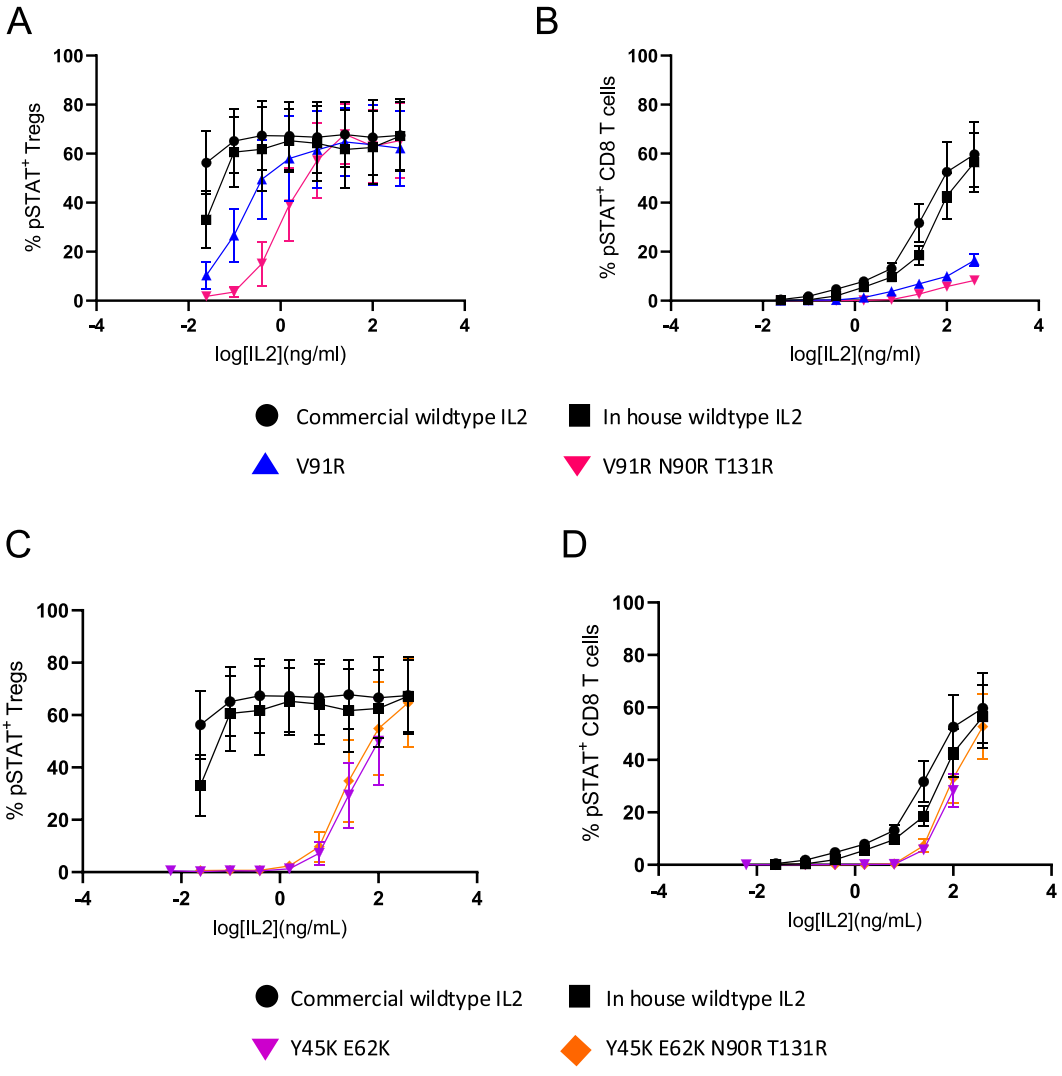

Fig. 7. Cellular selectivity of Human IL2 muteins is maintained with addition of production boosting mutations N90R and T131R. Human PBMCs were incubated for 20 minutes with either media containing IL2 or human Treg selective (A,B) or CD8 T cell selective (C,D) mutein, using a serial dilution of IL2 concentration, prior to staining for pSTAT5. A,C) The percentage of pSTAT5^{+} cells within the Treg or B,D) CD8 T cell populations (n=3). All muteins were tested in the same experiment using the same controls.

unfolding transitions.

Using the SolubiS method, human IL2 was identified to have two aggregation-prone regions, while the mouse IL2 only has one. The first aggregation-prone region in human IL2 can be broken by the N90R or N90E mutations. Interestingly, the N90R solution identified by SolubiS is the naturally-occurrent residue present in mouse IL2 (R125), indicating that the mouse has found the same gatekeeper solution of an arginine side-chain in this location. The second aggregation-prone region was predicted to be improved by T123N or T131R (human) or A138N or T146R (mouse). T146R showed production improvements in the mouse as a solo mutation. A138N improved production when in combination with V106R, while T146R was required to restore the production efficiency of N103H. In the human muteins, the N90E residue was detrimental to both production and functional activity, either in isolation or in combination with specificity-enhancing mutations. While the N90R, T131R and T123N mutations did not boost production alone, they helped boost production of the impaired Y45K, E62K and V91R proteins. In addition to the cost savings advantages that the aggregation-protecting mutations could deliver for IL2 production (a therapeutic protein with annual sales of US$60 million), the results here demonstrate the extension of the SolubiS method for improving recombinant cytokine production[43], [38], an area of growing therapeutic importance.

Beyond the biotechnology value of increasing protein production, here we used the SolubiS method to simultaneously improve both the production level and the functional properties of the native IL2 protein, through the introduction of single amino acid changes. This functional improvement is theoretically easier for the mutations designed to enhance specificity for CD8 T cells. As CD8 T cells generally do not express high levels of IL2RA, blocking IL2RA binding can substantially reduce Treg responses, while having negligible impact on CD8 T cell responses. Indeed, we have identified Y45K E62K (human) and Y59K (mouse) muteins which have simple cation-cation repulsion against the IL2RA, while maintaining signalling through IL2RB/IL2RG complexes. In addition, we have identified a murine CD8 T cell superkine Q30W with enhanced IL2RB binding, which, when combined with Y59K becomes a CD8 T cell superkine with greater cellular selectivity. These IL2RA independent IL2 muteins will be useful in stimulating responses in cells expressing the intermediate affinity dimeric receptor which includes both cytotoxic CD8 T cells and CD4 conventional T cells as well as other inflammatory cell types such as natural killer cells. By contrast, muteins to enhance specificity for Tregs face a potential “functionality tax”. While IL2 first binds IL2RA, the recruitment of IL2RB into the complex enhances signalling through the trimeric receptor. Thus, any mutations which completely block IL2RB binding will kill CD8 T cell responses, but also dampen down bioactivity on Tregs. Whilst maximal pSTAT5 signalling is not required for changes in Treg function, survival and fitness [44], maintaining good receptor bioactivity will likely reduce required doses. This “functionality tax” was observed on all Treg muteins, with the exception of V91R (human) / V106R (mouse) which were able to elicit maximal or near-maximal Treg responses, depending on the dose. The success of these muteins likely lies in the structure of IL2 being nearly identical whether free or bound to the receptor, with the exception of the beginning of helix C. Following binding to IL2RA, the beginning of helix C is slightly unwound to move forward by 1.0 Å, a confirmation change thought to prime superior binding to IL2RB via a hydrogen bond formed between N88 of IL2 and R42 of IL2RB [41]. In its unbound state, the IL2 muteins V106R (mouse) and V91R (human) exhibit a cation-cation repulsion to R41-R42, which blocks IL2RB binding. However, the binding of IL2 to IL2RA shifts the V106R / V91R residues back, enabling recruitment of IL2RB. This conformational-dependency of the V106R / V91R mutein effect may explain why interaction with CD8 T cells, via IL2RB, results in ~1000-fold reduction in signalling activity, whereas Tregs, which first require engagement of IL2RA, are still able to recruit IL2RB for full signalling capacity, eliciting maximal pSTAT5 responses in Tregs at the plateau dose. This advantage of specificity without loss of bioactivity is unlike that observed in some other Treg-specific muteins, where the loss of IL2RB binding is accompanied by an aggregate defect in signalling capacity even in Tregs where maximal Treg responses are not achieved [28,34,37]. The uniqueness of this solution also allows its potential combination with other mutations that directly enhance IL2RA binding [25], potentially creating a Treg superkine. Notably, V91R has been previously described as an IL2 antagonist [29]. We did not investigate competitive binding of V91R and wildtype IL2, but based on lack of signal in CD8 T cells, if V91R still binds IL2RB/IL2RG in a non-signalling conformation, it could potentially act as an antagonist in CD8 T cells, while acting as a bioactive signaller in Tregs. Fine-tuning the response to an IL2RA bias mutein is further complicated by the upregulation of IL2RA by activated CD8 and CD4 T cells, albeit to levels below that of Tregs competing for the same cytokine. Thus, under particular immunological contexts and dose ranges, even a fully IL2RA-restricted mutein could expansion opposing cell types. It is likely, however, that such contexts are less likely to arise during mutein treatment than wildtype IL2 treatment, as the lower doses used and the absence of initial feedback via IL2RBG limit IL2RA upregulation, while Treg expansion should heighten competition for the mutein.

By extending the study to include parallel engineering of mouse muteins, we have created a valuable research resource which will enable the study of specific T cell subset biology. Cellular selectivity boasts many advantages when studying T cell responses pre-clinically both in vivo and ex vivo by allowing expansion of specific T cell subsets. This is further enhanced by the increased production yield, meaning reagents are more readily available and easy to produce in useful quantities. Although the human muteins shown here are mostly cross-reactive, using mouse analogues can be helpful in pre-clinical safety and toxicity studies.

Using the combined computational method described here, 17 human candidates and 13 mouse candidates were identified, including candidates changes to residues of already know significance. Empirical testing of all candidates was performed and presented here, allowing overall success rates to be calculated. On single metric success rates, 38% of the muteins designed for greater stability exhibited improved production, while 90% and 92% of the muteins designed for loss of IL2RA or IL2RB interactions, respectively, demonstrated the desired properties. On a combined metric score, with multiple favourable properties identified, 3 successful candidates were taken forward from each species, resulting in a success rate of 17.6% and 23% respectively. Together, both the ability of the method to identify residues of significant importance and to produce successful muteins demonstrates the utility of incorporating SolibuS into affinity-based approaches when engineering cytokines and biologic therapeutics.

IL2 (marketed as Aldesleukin) was first approved for use in humans in 1992 using high doses to trigger CD8 T cell responses to aid tumour clearance in the treatment of renal carcinoma [45]. The short half-life of IL2, and low affinity for the IL2RB-IL2RG receptor, means large bolus doses were needed to reach the concentration needed to stimulate CD8 T cells. This resulted in severe side effects, such as capillary leak syndrome, being common in the initial clinical trials [46], and tumour clearance efficacy inferior to that later observed with immune checkpoint blockade. Since this early clinical use, the conceptual shift in our understanding of IL2 biology warranted re-orientation of the drug for anti-inflammatory use. As such, clinical trials have been run using multiple low-doses of IL2 to successfully at elevate Treg numbers in inflammatory conditions such as Graft Versus Host Disease and Systemic Lupus Erythematosus amongst others [47–50]. Although trials have shown success in reducing disease symptoms, dosing remains a challenge due to the small therapeutic window. The muteins discussed here may help fix many of the caveats of IL2 therapy. Firstly, increased production efficiency of IL2 will help reduce costs making therapies more accessible to patients. Secondly increased specificity of the muteins will help ameliorate some of the side effects. It can be

hypothesised that due to the selectivity of muteins Y45K E62K and Y45K E62K N90R T131R for CD8 T cells, lower doses may stimulate effective CD8 T cell responses, while simultaneously reducing the risk of severe side effects and increasing protein half-life due to less consumption by off-target Tregs. Likewise, but with an inverted hierarchy of specificity, the V91R or V91R N90R T131R muteins, with enhanced selectivity for Tregs, may further decrease the dose required to elicit therapeutic Treg responses. By combining selective IL2 muteins like those discussed here with novel delivery systems such as AAVs, which allow stable, tissue specific protein production [20], we can address many of the limiting characteristics of IL2 therapy, such as half-life, therapeutic window and off-target responses. Together these approaches have the potential to further enhance the efficacy of IL2 in the clinic for both anti- and pro-inflammatory uses.

4. Materials and methods

4.1. IL2 mutation design

Mutations were designed based on four structures of human IL2: 1m47 (IL2 alone, resolution of 1.99 Å [51]), 1z92 (IL2 with IL2RA, resolution of 2.8 Å [52]), 2b5i (IL2 with IL2RA/IL2RB/IL2RC, resolution of 2.3 Å [41]) and 2erj (IL2 with IL2RA/IL2RB/IL2RC, resolution of 3 Å [53]), and one structure of mouse IL2: 4yqx (IL2 bound to anti-IL2 single chain Fv, resolution of 2.8 Å [18]). Mutation design was based on the SolubiS method [54–56] to predict aggregation-prone regions from the primary peptide sequence. The thermodynamic contribution of these regions to the stability of the protein was predicted using FoldX [57], an empirical force field developed for the rapid evaluation of the effect of mutations, and TANGO, a statistical thermodynamics algorithm [55]. TANGO calculates the intrinsic aggregation propensity of aggregation-prone regions using a Boltzmann distribution with competing secondary structural tendencies, such as α-helical or β-hairpin structure. The benefit of this implementation is that TANGO predicts aggregation-prone regions [54] with well-defined sequence boundaries, with high specificity and thus predicts few false positives [58]. Each amino acid of the wildtype IL2 protein was mutated to every other amino acid in each structure. The effect of both the thermodynamic stability (ddG) as well as the stability of the interaction (ddG_complex) with each of the receptors was calculated using FoldX (version 3.0 beta 6), and the effect of each mutation on the aggregation propensity was calculated using TANGO, based on sequence alone. This analysis resulted in a large table of FoldX energies and aggregation propensity (TANGO) scores. Mutations were selected using four strategies: SolubiS (reducing aggregation while retaining stability), kill IL2RA binding (reducing interaction energy with IL2RA, while retaining stability and preferably reducing aggregation), kill IL2RB binding (reducing interaction energy with IL2RB, while retaining stability and preferably reducing aggregation), and combinations (identifying synergies that combine aggregation reduction and IL2RA/IL2RB binding). The thresholds used were reduction of TANGO score by more than 100, for reduction in aggregation, while not destabilising hIL2 thermodynamically (ddG < 0.5 kcal/mol) and not affect any receptor interactions negatively (ddG_complex < 0.5 kcal/mol). These single point mutations were calculated in combination to allow for the previously described synergistic effect of SolubiS mutations on the aggregation resistance of proteins [40]. These mutation combinations were selected in the same way as single SolubiS mutations, to ensure compatibility.

Structural models of IL2 in complex with the trimeric receptor were based off the 2erj structure [53] of the human IL2 / IL2R complex. Due to the high homology between mouse and human IL2 and IL2R complex, and the lack of a mouse structure, selected human mutations were directly imposed on the mouse sequence. Each introduced amino acid was the same for both human and mouse mutant. This resulted in some cases where a different wildtype amino acid was mutated to the same mutant amino acid. For example, in the case of the H16W mutation, where the human homologue has a histidine residue, the mouse homologue has a glutamine residue, making the mouse equivalent mutant Q30W. FoldX calculations were performed on the monomeric crystal structure 4yqx (mIL2 alone, resolution 2.8 Å [18]).

4.2. Cloning and molecular biology

IL2 muteins were ordered as Gene Fragments from GeneWiz, Azenta. Gene Fragments were cloned into pJet Blunt 1.2 (ThermoFisher, K1231) and sequenced via Sanger Sequencing (Genewiz, Azenta) to confirm correct sequence insertion. Correct insertions were amplified via PCR adding restriction enzyme sites to each end. PCR products were purified using GeneJET PCR purification kit (ThermoFisher, K0701) before being digested with Pfl23II (ThermoFisher, FD0854) and *Nde*I (ThermoFisher, FD0583) and gel purified (GeneJET Gel Extraction Kit, ThermoFisher, K0691) to obtain the IL2 sequence. For low-expressing murine muteins V106R, N103H T146R and Y59K E76K T146R, codon-optimised sequences were used. Fragments were then cloned into an expression vector, downstream of an EF-1α promoter and in frame with a TEV protease target and a 6xHis-Tag. Finally, sequences were confirmed using Sanger sequencing (Genewiz, Azenta).

4.3. IL2 production and measurement

Expression plasmids were transfected into HEK293 cells, seeded at 100,000 cells/well, using FuGENE HD Transfection reagent (Promega, E2311) in 24 well plates containing 500 μL DMEM supplemented with 10% FBS. 24 hours following transfection, wells were topped with an additional 250 μL of DMEM, 10% FBS. After a total of 48 hours, the culture supernatant containing IL2 protein was harvested and frozen at -80ºC. All supernatants were aliquoted prior to freezing to prevent multiple freeze thaw cycles. The cells were washed with PBS and detached, and cell pellets were frozen at -80ºC ready for DNA extraction. Transduction efficiency was calculated through PCR quantification of the vector. DNA was extracted from frozen cell pellets using the DNeasy Blood and Tissue Kit (Qiagen, 69504) following manufacturer's instructions. DNA samples were analysed using QuantStudio 1 via qPCR using TaqMan Gene Expression Assays (FAM) for the detection of plasmid DNA (using the neomycin resistance cassette) relative to genomic DNA detection of GAPDH (Hs02786624_g1) and PPIA (Hs04194521_s1), enabling the transfection efficiency to be calculation for production normalisation.IL2 production was analysed via a modified sandwich ELISA. Plates were coated with anti-IL2 antibodies ((mouse: clone JES6–1A12, BioLegend, 503701) (human: polyclonal, Bio-Techne, AF-202-NA)). The detection antibody was HRP-conjugated anti-Histag (BioLegend, 652503). Standard curves were created using his-tagged IL2 (GeneTex: Mouse; GTX00285-pro, Human; GTX00092-pro), from which concentrations of IL2 in cell culture supernatant were interpolated. To compare production efficiency of each IL2 mutein, final concentrations were normalised by transfection efficiency values calculated from aforementioned qPCR.

4.4. Phospho- STAT Flow cytometry

For murine phospho-STAT assays, spleens dissected from C57Bl/6 mice were mechanically disrupted between two glass slides, filtered through 100 μm mesh and red blood cells lysed to form single cell suspensions. Cell suspensions were counted using a CellDrop cell counter. Non-specific binding was blocked using 2.4G2 supernatant. Surface staining was performed with antibodies against CD4, CD127, CD62L, CD25, CD44 as well as an e780 fixable Live-Dead stain (eBioscience). Splenocytes were then stimulated with wildtype IL2 and mutated IL2 diluted to a range of concentrations (400–0.02 ng/ml) in complete DMEM. Immediately following stimulation, cells were fixed with paraformaldehyde followed by methanol. An overnight stain [59] was then preformed with antibodies against Foxp3, CD3, CD8, pSTAT5, CD122,

CD132 and pSTAT3. Following staining, data was acquired on a Cytek Aurora, with data collection performed in SpectroFlo (Cytek) and analysed using FlowJo and GraphPad Prism.

For human phospho-STAT assays, PBMCs were isolated from leukocytes cones from healthy donors (NHSBT NCI) using Ficoll, following the manufacturer's instructions. Cell suspensions were counted using a CellDrop cell counter. Non-specific binding was blocked using FcX Trustain (1:200) (BioLegend). Surface staining was performed with antibodies against CD4, CD3, CD8, CCR7, CD45RA, CD27, CD56 as well as an e780 fixable live dead stain (eBioscience). Cells were then stimulated with wildtype and mutant IL2, diluted to a range of concentrations (400–0.02 ng/ml) in complete DMEM. Immediately following stimulation, cells were fixed with paraformaldehyde followed by methanol. An overnight stain [59] was the performed with antibodies against FOXP3, CD25, and pSTAT5. Following staining, data was acquired on a Cytek Aurora, with data collection performed in SpectroFlo (Cytek) and analysed using FlowJo and GraphPad Prism.

4.5. In vivo gene delivery and assessment

For gene therapy studies using adeno-associated virus-based vectors (AAVs) male and female C57BL/6 wildtype mice were obtained from Babraham Institute Biological Support Unit. All mice were maintained in a specific pathogen free environment, with ambient temperature, humidity, and lighting maintained for their well-being. Before experimentation, mice were transferred to individually-ventilated cages, and grouped matching age and sex. Mice were fed with either wet or dry standard food pellets based on the animal food consumption preferences.

Wildtype (C57BL/6) mice were intranasally inoculated with 50 μL of 1×10^{11} GC/ml of AAVs diluted in PBS. All mouse experimentation and procedures compiled with the UK Home Office guidelines observing the Animals Scientific Procedures Act 1986. Experiments were also approved by the Babraham Institute Animal Welfare and Ethical Review Body (Protocol study number PP3981824- Lymphocyte development and immune function in the tissues).

rAAV constructs were created using AAV6.2 capsid and Scgb1a1 promoter. The expressed gene was GFP-Myc-Cre (Addgene #49056), murine IL2 (NM_008366.3) or murine IL2 V106R (GTA to AGA in codon 126). Vectors were produced by Vector Builder (sterile, <90% purity).

At the indicated time points post-treatment, mice were injected intravenously with anti-CD45 antibody before euthanasia. The lung was harvested into PBS with 2.5% FCS and 2 mM EDTA. Tissues were homogenized in Protein Quant Sample Lysis kit Thermo Scientific™ buffer and a protease inhibitor (Complete Mini EDTA Sigma). The resultant supernatant was checked for IL2 levels using ProQuantum High-Sensitivity Immunoassays Kit from Thermo Fisher following the manufacturer's protocol. IL2 standard curves were done on the ProQuantum platform (Thermo Scientific).

For flow cytometry analysis, tissues were processed as previously described [60]. Samples were prepared by initially blocking Fc interactions with supernatant from 2.4 G2 hybridoma cell lines, followed by viability staining, staining with the surface marker cocktail for 2 hours, and staining overnight for intracellular markers [59] (Supplementary Table 1). 10,000 Precision Count beads (BioLegend) were added to samples before running through a Cytek™ Aurora (5 Lasers N9–20001_Spectral). Data analysis, including flow cytometry gating, was performed with FlowJo v.10.0.7 and FlowJo version 10.8.1 (BD).

Funding

The work was supported by the VIB, an ERC Proof of Concept Grant TreatBrainDamage (to A.L.), the Biotechnology and Biological Sciences Research Council through Institute Strategic Program Grant funding BBS/E/B/000C0427 and BBS/E/B/000C0428, and the Biotechnology and Biological Sciences Research Council Core Capability Grant to the Babraham Institute. MGH is currently the ERANet Chair (NCBio) at i3S Porto funded by the European Commission (H2020-WIDESPREAD-2018–2020–6; NCBio; 951923).

CRediT authorship contribution statement

Dooley James: Supervision, Data curation, Conceptualization. **Burton Oliver:** Methodology. **Lienart Stephanie:** Visualization, Data curation. **Hernandez Alvaro R:** Data curation. **Kouser Lubna:** Data curation. **Ali Magda:** Data curation. **Naranjo Francisco:** Data curation. **Liston Adrian:** Writing – review & editing, Writing – original draft, Supervision, Funding acquisition, Conceptualization. **Ghodsinia Arman:** Data curation. **Schymkowitz Joost:** Supervision, Conceptualization. **van der Kant Rob:** Investigation, Formal analysis, Data curation. **Rousseau Frederic:** Supervision, Conceptualization. **Makuyana Ntombizodwa:** Formal analysis, Data curation. **Holt Matthew G:** Writing – review & editing, Conceptualization. **Dashwood Amy:** Writing – review & editing, Writing – original draft, Investigation, Formal analysis, Data curation.

Conflict of Interest

The University of Cambridge, VIB and Babraham Institute are owners of a pending patent application based on work included in the manuscript, with the authors being potential financial beneficiaries of commercialization. The VIB are owners of patent EP2839001B1 on the SolubiS method, with VIB authors financial beneficiaries of commercialization.

Acknowledgments

The authors acknowledge the important contributions of the Babraham Institute Flow Cytometry Core and Biological Services Unit and the University of Cambridge FACS Core and University Biological Services Unit.

Appendix A. Supporting information

Supplementary data associated with this article can be found in the online version at doi:10.1016/j.csbj.2025.03.002.

Data availability statement

All data are available in the main text or the supplementary materials.

References

[1] Malek TR. The biology of interleukin-2. Annu Rev Immunol 2008;26:453–79.
[2] Pierson W, et al. Antiapoptotic Mcl-1 is critical for the survival and niche-filling capacity of Foxp3+ regulatory T cells. Nat Immunol 2013;14:959–65.
[3] Shi H, et al. Hippo kinases Mst1 and Mst2 sense and amplify IL-2R-STAT5 signaling in regulatory T cells to establish stable regulatory activity. e896 Immunity 2018; 49:899–914. e896.
[4] Obata Y, et al. The epigenetic regulator Uhrf1 facilitates the proliferation and maturation of colonic regulatory T cells. Nat Immunol 2014;15:571–9.
[5] Fontenot JD, Rasmussen JP, Gavin MA, Rudensky AY. A function for interleukin 2 in Foxp3-expressing regulatory T cells. Nature Immunology 2005;6:1142–51.
[6] Spangler JB, Moraga I, Mendoza JL, Garcia KC. Insights into cytokine–receptor interactions from cytokine engineering. Annual Review Immunology 2015;33: 139–67.
[7] Liston A, Gray DH. Homeostatic control of regulatory T cell diversity. Nat Rev Immunol 2014;14:154–65.
[8] Amado IF, et al. IL-2 coordinates IL-2-producing and regulatory T cell interplay. J Exp Med 2013;210:2707–20.
[9] Whyte CE, et al. Context-dependent effects of IL-2 rewire immunity into distinct cellular circuits. J Exp Med 2022;219.
[10] Humblet-Baron S, et al. IL-2 consumption by highly activated CD8 T cells induces regulatory T-cell dysfunction in patients with hemophagocytic lymphohistiocytosis. e208 J Allergy Clin Immunol 2016;138:200–9. e208.

[11] Humblet-Baron S, et al. IFN-γ and CD25 drive distinct pathologic features during hemophagocytic lymphohistiocytosis. e2217 J Allergy Clin Immunol 2019;143:2215–26. e2217.
[12] Donohue JH, Rosenberg SA. The fate of interleukin-2 after in vivo administration. J Immunol 1983;130:2203–8.
[13] Lotze MT, Frana LW, Sharrow SO, Robb RJ, Rosenberg SA. In vivo administration of purified human interleukin 2. I. Half-life and immunologic effects of the Jurkat cell line-derived interleukin 2. J Immunol 1985;134:157–66.
[14] Yang JC, et al. The use of polyethylene glycol-modified interleukin-2 (PEG-IL-2) in the treatment of patients with metastatic renal cell carcinoma and melanoma. A phase I study and a randomized prospective study comparing IL-2 alone versus IL-2 combined with PEG-IL-2. Cancer 1995;76:687–94.
[15] Zhang B, et al. Site-specific PEGylation of interleukin-2 enhances immunosuppression via the sustained activation of regulatory T cells. Nat Biomed Eng 2021;5:1288–305.
[16] Vazquez-Lombardi R, et al. Potent antitumour activity of interleukin-2-Fc fusion proteins requires Fc-mediated depletion of regulatory T-cells. Nature Commun 2017;8:15373.
[17] Orcutt-Jahns BT, Emmel PC, Snyder EM, Taylor SD, Meyer AS. Multivalent, asymmetric IL-2-Fc fusions show enhanced selectivity for regulatory T cells. Sci Signal 2023;16:eadg0699.
[18] Spangler JB, et al. Antibodies to interleukin-2 elicit selective T cell subset potentiation through distinct conformational mechanisms. Immunity 2015;42:815–25.
[19] Ward NC, et al. IL-2/CD25: a long-acting fusion protein that promotes immune tolerance by selectively targeting the IL-2 receptor on regulatory T cells. J Immunol 2018;201:2579–92.
[20] Yshii L, et al. Astrocyte-targeted gene delivery of interleukin 2 specifically increases brain-resident regulatory T cell numbers and protects against pathological neuroinflammation. Nature Immunol 2022;23:878–91.
[21] Rojas G, et al. Directed evolution of super-secreted variants from phage-displayed human Interleukin-2. Scientific Rep 2019;9:800.
[22] Levin AM, et al. Exploiting a natural conformational switch to engineer an interleukin-2 'superkine. Nature 2012;484:529–33.
[23] Ren J, et al. Interleukin-2 superkines by computational design. Proc Natl Acad Sci USA 2022;119:e2117401119.
[24] Glassman CR, et al. Calibration of cell-intrinsic interleukin-2 response thresholds guides design of a regulatory T cell biased agonist. Elife 2021;10.
[25] Rao BM, Girvin AT, Ciardelli T, Lauffenburger DA, Wittrup KD. Interleukin-2 mutants with enhanced alpha-receptor subunit binding affinity. Protein Eng 2003;16:1081–7.
[26] Carmenate T, et al. Human IL-2 mutein with higher antitumor efficacy than wild type IL-2. J Immunol 2013;190:6230–8.
[27] Rojas G, et al. Molecular reshaping of phage-displayed Interleukin-2 at beta chain receptor interface to obtain potent super-agonists with improved developability profiles. Commun Biol 2023;6:828.
[28] Khoryati L, et al. An IL-2 mutein engineered to promote expansion of regulatory T cells arrests ongoing autoimmunity in mice. Sci Immunol 2020;5.
[29] Liu DV, Maier LM, Hafler DA, Wittrup KD. Engineered interleukin-2 antagonists for the inhibition of regulatory T cells. J Immunother 2009;32:887–94.
[30] Mitra S, et al. Interleukin-2 activity can be fine tuned with engineered receptor signaling clamps. Immunity 2015;42:826–38.
[31] Carmenate T, et al. Blocking IL-2 signal in vivo with an IL-2 antagonist reduces tumor growth through the control of regulatory T cells. J Immunol 2018;200:3475–84.
[32] Mo F, et al. An engineered IL-2 partial agonist promotes CD8(+) T cell stemness. Nature 2021;597:544–8.
[33] Chen AC, et al. A Treg-Selective IL-2 mutein prevents the formation of factor viii inhibitors in hemophilia mice treated with factor VIII gene therapy. Front Immunol 2020;11:638.
[34] Lu DR, et al. Dynamic changes in the regulatory T-cell heterogeneity and function by murine IL-2 mutein. Life Sci Alliance 2020;3.
[35] Silva DA, et al. De novo design of potent and selective mimics of IL-2 and IL-15. Nature 2019;565:186–91.
[36] Sockolosky JT, et al. Selective targeting of engineered T cells using orthogonal IL-2 cytokine-receptor complexes. Science 2018;359:1037–42.
[37] de Picciotto S, et al. Selective activation and expansion of regulatory T cells using lipid encapsulated mRNA encoding a long-acting IL-2 mutein. Nat Commun 2022;13:3866.
[38] van der Kant R, et al. Prediction and reduction of the aggregation of monoclonal antibodies. J Mol Biol 2017;429:1244–61.
[39] Castillo V, Ventura S. Amyloidogenic regions and interaction surfaces overlap in globular proteins related to conformational diseases. PLoS Comput Biol 2009;5:e1000476.
[40] van der Kant R, van Durme J, Rousseau F, Schymkowitz J. SolubiS: optimizing protein solubility by minimal point mutations. Methods Mol Biol 2019;1873:317–33.
[41] Wang X, Rickert M, Garcia KC. Structure of the quaternary complex of interleukin-2 with its alpha, beta, and gammac receptors. Science 2005;310:1159–63.
[42] Mosmann TR, et al. Species-specificity of T cell stimulating activities of IL 2 and BSF-1 (IL 4): comparison of normal and recombinant, mouse and human IL 2 and BSF-1 (IL 4). J Immunol 1987;138:1813–6.
[43] Ganesan A, et al. Structural hot spots for the solubility of globular proteins. Nat Commun 2016;7:10816.
[44] Ghelani A, et al. Defining the threshold IL-2 signal required for induction of selective treg cell responses using engineered IL-2 muteins. Front Immunol 2020;11:1106.
[45] McDermott DF, et al. The high-dose aldesleukin "select" trial: a trial to prospectively validate predictive models of response to treatment in patients with metastatic renal cell carcinoma. Clin Cancer Res 2015;21:561–8.
[46] Schwartz RN, Stover L, Dutcher JP. Managing toxicities of high-dose interleukin-2. Oncology (Williston Park) 2002;16:11–20.
[47] Whangbo JS, et al. Dose-escalated interleukin-2 therapy for refractory chronic graft-versus-host disease in adults and children. Blood Adv 2019;3:2550–61.
[48] Kennedy-Nasser AA, et al. Ultra low-dose IL-2 for GVHD prophylaxis after allogeneic hematopoietic stem cell transplantation mediates expansion of regulatory T cells without diminishing antiviral and antileukemic activity. Clin Cancer Res 2014;20:2215–25.
[49] La Cava A. Low-dose interleukin-2 therapy in systemic lupus erythematosus. Rheumatol Immunol Res 2023;4:150–6.
[50] Humrich JY, et al. Low-dose interleukin-2 therapy in refractory systemic lupus erythematosus: an investigator-initiated, single-centre phase 1 and 2a clinical trial. Lancet Rheumatol 2019;1:e44–54.
[51] Arkin MR, et al. Binding of small molecules to an adaptive protein-protein interface. Proc Natl Acad Sci USA 2003;100:1603–8.
[52] Rickert M, Wang X, Boulanger MJ, Goriatcheva N, Garcia KC. The structure of interleukin-2 complexed with its alpha receptor. Science 2005;308:1477–80.
[53] Stauber DJ, Debler EW, Horton PA, Smith KA, Wilson IA. Crystal structure of the IL-2 signaling complex: paradigm for a heterotrimeric cytokine receptor. Proc Natl Acad Sci USA 2006;103:2788–93.
[54] Rousseau F, Schymkowitz J, Serrano L. Protein aggregation and amyloidosis: confusion of the kinds? Curr Opin Struct Biol 2006;16:118–26.
[55] Fernandez-Escamilla AM, Rousseau F, Schymkowitz J, Serrano L. Prediction of sequence-dependent and mutational effects on the aggregation of peptides and proteins. Nat Biotechnol 2004;22:1302–6.
[56] Linding R, Schymkowitz J, Rousseau F, Diella F, Serrano L. A comparative study of the relationship between protein structure and beta-aggregation in globular and intrinsically disordered proteins. J Mol Biol 2004;342:345–53.
[57] Schymkowitz J, et al. The FoldX web server: an online force field. Nucleic Acids Res 2005;33:W382–8.
[58] Hamodrakas SJ. Protein aggregation and amyloid fibril formation prediction software from primary sequence: towards controlling the formation of bacterial inclusion bodies. Febs j 2011;278:2428–35.
[59] Whyte CE, Tumes DJ, Liston A, Burton OT. Do more with less: improving high parameter cytometry through overnight staining. Curr Protoc 2022;2:e589.
[60] Burton OT, et al. The tissue-resident regulatory T cell pool is shaped by transient multi-tissue migration and a conserved residency program. e1510 Immunity 2024;57:1586–602. e1510.